Effects of Surface Radiation on the Unsteady Natural Convection in a Rectangular Enclosure

Seung-Wook Baek*
Department of aerospace engineering
Korea advanced institute of science and technology
Daejon City, Korea 373-1

Taig-Young Kim**
Department of mechanical engineering
Korea polytechnic university
Shihung City, Korea 429-450

Abstract

Numerical solution of the full Navier-Stokes equation as well as the energy equation has been obtained for the unsteady natural convection in a rectangular enclosure. One side wall was maintained at very high temperature simulating fires. Especially the effect of surface radiation was taken into account. While the enclosed air was assumed to be transparent, the internal walls directly interacted one another through the surface radiation. Due to a significant temperature difference in the flow field, the equation of state was used instead of the Boussinesq approximation. It was found that the rapid heating of the adiabatic ceiling and floor by the incoming radiation from the hot wall made the evolution at thermo-fluid field highly unstable in the initial period. Therefore, the secondary cells brought about at the floor region greatly affected the heat transfer mechanism inside the enclosure. The heat transfer rate was augmented by the radiation, resulting in requiring less time for the flow to reach the steady state. At the steady state neglecting radiation two internal hydraulic jumps were clearly observed in upper/left as well as in lower/right corner. However, the hydraulic jump in the lower/right corner could not be observed for the case including radiation due to its high momentum flow over the bottom wall. Radiation resulted in a faster establishment of the steady state phenomena

Key Word : unsteady natural convection, surface radiation

Introduction

Buoyancy induced convective fluid flow in a confined enclosure is a long-standing topic in the area of heat and mass transfer due to a number of diverse physical applications such as thermal insulation in buildings, unexpected hostile fire hazard, solar energy collection system, thermal mode of nuclear reactors, chip cooling in electronic or computer equipment, crystal growth for the semiconductor and convective processes in lakes, oceans, and magma chambers. Accordingly there have been numerous theoretical, experimental, and numerical studies of various aspects of the natural convective flow.

* Professor
** Assistant Professor
E-mail : tagikim@kpu.ac.kr, TEL : 031-496-8206, FAX : 031-496-8219

In the past several decades many researches have been done to solve both steady[1-5] and unsteady[6-10] natural convective problems. Based on these works, an oscillatory mode of solution, while converging to a final steady state, was found to exist for certain flow conditions. This oscillatory behavior is theorized to result from due to the momentum inertia of the flow entering the interior of cavity from the side wall boundary layers, which can also lead to a phenomenon of hydraulic jump if the Rayleigh number ($Ra = g\beta TH^3/\nu\alpha$) is sufficiently large.

Whereas most of the aforementioned works were performed under the circumstance of a slight temperature difference between two differently heated end walls, there are many practical problems related to various types of heating of internal walls or the high wall temperature difference in a confined geometry. Chen et al.[11] studied a buoyancy induced flow in a rectangular enclosure with differently heated walls while the floor is always kept at a low temperature. Steady natural convection in a rectangular cavity with differentially heated end walls with a local heat source at the floor has been investigated by Zia et al.[12]. It was found that there could exist several types of flow pattern depending on the redefined Rayleigh number which reflects the equivalent relative intensity of local heat source. When the intensity of internal heat source is quite strong enough compared with the external heating from the heated vertical wall, the uprising flow motion is brought about and it makes the two secondary cells located in left and right-hand side of this uprising flow. Recently Hasnaoui et al.[13] numerically examined the natural convection in a rectangular enclosure composed of adiabatic vertical walls, floor with partial heating, and cold ceiling. Given appropriate initial perturbations, multiple solutions including two-cell convection were observed for the steady state case. The periodic as well as non-periodic chaotic behavior was also discussed for the various parameters.

If a wall is maintained at a very high temperature, the surface wall radiation may play an important role even if the participating medium is not radiatively active. Sometimes this surface radiation among the walls of the confined enclosure can greatly affect the basic nature of internal flow pattern and a totally different flow situation could be obtained compared with the case with no radiation. The rapid heating of walls by incident radiation, in particular the bottom wall, would make the flow locally unstable because of its buoyancy effect, so that a very complicated fluid motion could be incurred during an initial developing period. This might enhance the thermo-fluid field development and promote the internal heat transfer process. Subsequently it can reduce the time for the flow to reach its steady state. Larson and Viskanta[14] studied the transient natural convection in which the surface radiation was taken into account. The governing equations were cast in the form of stream function and vorticity. Additionally the Boussinesq approximation was adopted. Their solution was then obtained for two orders lower Rayleigh number than that studied here. Consequently, it resulted in much simpler flow development inside the enclosure and thus the very complex uprising flow motion, usually observed in developing period, could not be detected.

In present study the problem of unsteady natural convection in a rectangular enclosure is numerically investigated by solving both the full Navier-Stokes equation and energy equation in the form of primitive variables. Instead of the Boussinesq approximation, more relaxed equation of state is used here. In the Boussinesq approximation, except for the buoyancy term the density is regarded as constant in all the other terms such as time and convective derivatives. This might cause serious errors in predicting a flow development, especially at a high temperature zone in which the density is inversely proportional to temperature. This is the case of present study in which a compressible air is used as a working fluid. In addition, full temperature dependencies of physical properties are taken into account here. Whereas the enclosed air is considered transparent, the internal surface walls can directly interact each other through the surface radiation.

Analysis

The schematic diagram and physical coordinate system for the theoretical model are represented in Fig. 1. At $t > 0$, the left-hand side wall temperature is suddenly elevated to a

higher value temperature and remained as such. While the ceiling and floor are assumed to be insulated both radiation and conduction, the right-hand side wall is kept at 300 K. Due to its large temperature difference the air experiences, the equation of state for ideal gas is used instead of the Boussinesq approximation. Furthermore, the pressure work and dissipation terms are not neglected here. However, the two-dimensional laminar flow is assumed and thus the Rayleigh number is chosen to be 5.6×10^{7}.

According to these assumptions, the governing equations can be expressed as follows:

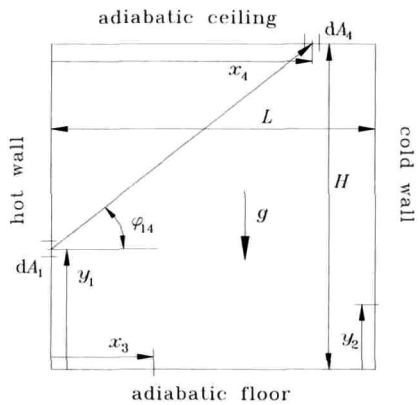

Fig. 1 Schematic diagram of the physical domain and its coordinates

$$\frac{\partial\rho}{\partial t}+\nabla\cdot(\rho v)=0 \tag{1}$$

$$\rho\frac{\partial v}{\partial t}+\rho v\cdot\nabla v=-\nabla p+\nabla\cdot\tau_{ij}+\rho g \tag{2}$$

$$\rho\frac{\partial h}{\partial t}+\rho v\cdot\nabla h=\nabla\cdot(\lambda\nabla T)+\frac{\partial p}{\partial t}+v\cdot\nabla p+\Phi \tag{3}$$

where τ_{ij} and Φ are stress tensor and dissipation function, respectively. Since the air is considered perfect gas, the equation of state for ideal gas is given by

$$p=R\rho T. \tag{4}$$

The following temperature-dependent transport properties of air are used[15].

$$\mu=\frac{14.58\times10^{-7}T^{3/2}}{110.4+T}\quad[\text{kg/ms}] \tag{5}$$

$$\lambda=\frac{2.6482\times10^{-3}T^{1/2}}{1+245.4\times10^{-12/T}/T}\quad[\text{W/mk}] \tag{6}$$

$$C_p=0.917+2.58\times10^{-4}T-3.98\times10^{-8}T^{2}\quad[\text{kJ/kg/K}] \tag{7}$$

To keep the flow in laminar regime, the height and length of the rectangular enclosure are 0.1 m respectively. Initially the air and all the wall temperatures are held at 300 K and the air is stagnant. On the wall boundary no-slip condition is applied. The boundary condition for the energy equation at the adiabatic ceiling and floor is

$$q_w^T=q_w^C+q_w^R=0 \tag{8}$$

Therefore, the radiative and conductive heat fluxes have opposite signs on the adiabatic wall.

In this work, since the direct exchange of radiative energy is assumed among the gray walls involved, it is necessary to account for the radiative heat flux at each wall. The radiative heat flux at the j-th gray wall with an arbitrary temperature distribution can be written by

$$q_j^R(s)=J_j(s)-G_j(s) \tag{9}$$

where q^R, G, and J represent the net radiative flux, irradiation, and radiosity at the surface, respectively. There is the following relation between irradiation and radiosity:

$$q_j^R(s)=\varepsilon_j\sigma T_j^4(s)+(1-\varepsilon_j)G_j(s) \tag{10}$$

$$dA_jG_j(s)=\sum_{i=1}^{4}\int_{A_i}J_i(s)\,dF_{i-j}dA_i \tag{11}$$

where ε_j, dA_j, and dF_{i-j} are the wall emissivity, differential area of the j-th wall and geometric configuration factor defined as a fraction of energy leaving the elemental surface area dA_i that arrives at the surface element dA_j. A black body is assumed for wall emissivity. From equations (9), (10), (11), and the reciprocity relation governing the geometric configuration factors, the following relations can be obtained.

$$J_j(s) = \varepsilon_j \sigma T_j^4(s) + (1-\varepsilon_j) \sum_{i=1}^{4} \int_{A_i} J_i(s)\, dF_{j-i} \tag{12}$$

$$q_j^R(s) = \frac{\varepsilon_j}{1-\varepsilon_j} [\sigma T_j^4(s) - J_j(s)] \tag{13}$$

According to the physical coordinates in Fig. 1, the geometric configuration factors can be deduced from the following relation[16].

$$dF_{j-i} = \frac{1}{2} \cos \Phi_{ij}\, d\Phi_{ij} \tag{14}$$

The governing equations are numerically solved with the primitive variables. The fully implicit discretization is employed for the time difference, the central differencing scheme for the diffusive and source terms, and the generalized QUICK scheme[17] for the convective term. The gas phase governing equations are solved by the SIMPLER algorithm[18]. The algebraic equations for the discretized form of radiative exchange are solved by direct inversion of the full matrix. A 61×61 non-uniform grid is adopted for the gas phase calculation, with more

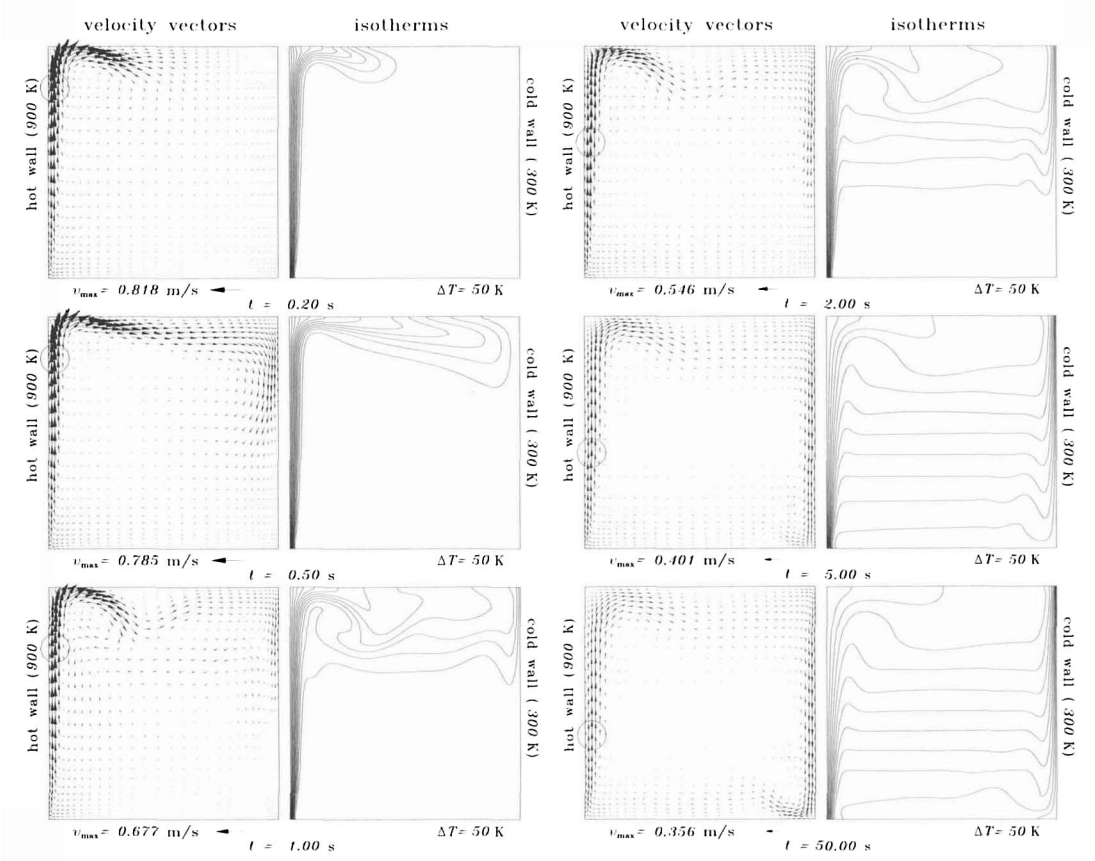

Fig. 2. Temporal variation of velocities and isotherms for the case without radiation

computational cells clustered near the wall region. There is no dramatic distinctions between the computational results with this grid system and with the denser grid systems. Very small time step in the initial developing period is employed to resolve the uprising flow patterns. After the removal of flow instability the longer time step is used for expediting the computation.

Results and Discussion

The solution accuracies are compared with the experimental data of steady state under the moderate Rayleigh number, and there are good agreement between them. In order to discuss the effect of surface radiation on the evolution of internal thermo-fluid field, it is necessary to examine the case without radiation first. All the results were obtained with left-hand side wall temperature of 900 K and right-hand side wall temperature of 300 K. The ceiling and floor are

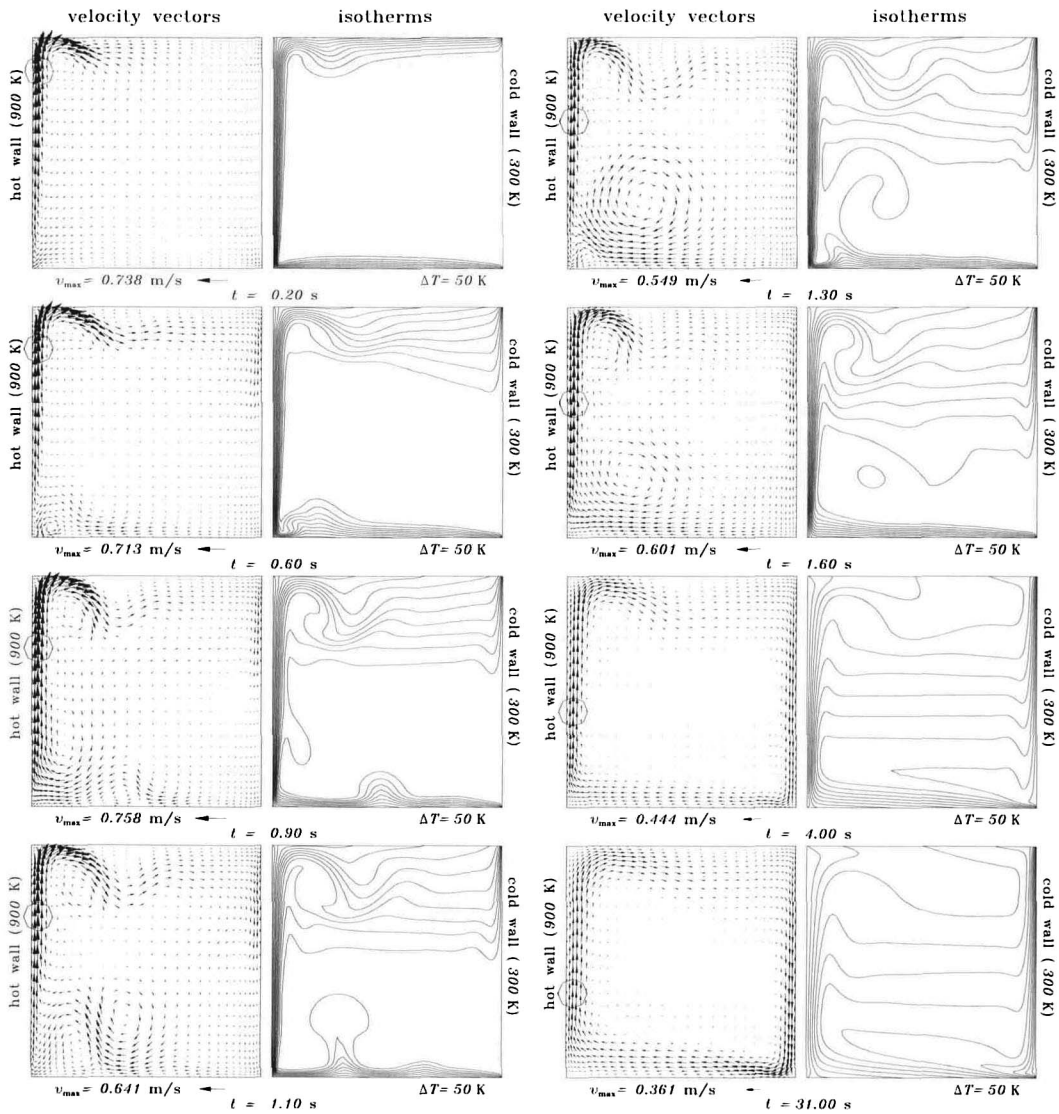

Fig. 3. Temporal variation of velocities and isotherms for the case with radiation

insulated against both radiation and conduction.

Figure 2 shows the temporal of thermo-fluid field until a steady state is reached. Initially a very steep temperature gradient is shown to be formed along the hot wall by conduction only, since the radiation is not involved. As this temperature gradient induces the free convective boundary layer, the heated air begins to infiltrate the upper zone along the adiabatic ceiling. As the upward flow is getting stronger, it turns in a downward direction due to blockage by the ceiling wall. Especially when it bounces off the ceiling as shown at $t=1.0$s, it is called the hydraulic jump. Simultaneously, a small clockwise recirculation zone is generated in the upper/left corner through $t=2.0$s and then disappears afterwards. The heated air originating from the hot wall turns again downward along the cold right-hand side wall. As time passes on, the thermal field becomes horizontally stratified in the inner zone. At the same time the velocity and thermal boundary layers are constructed along both side walls. After 20s there is no noticeable change in the velocity and temperature distributions. As a criterion of the steady state in this study, a relation $\partial \overline{Nu}_{net}^{T} / \partial t < 0.001$ is used. For the physical conditions given above, it takes 30s for the steady state to be reached. At steady state the internal flow does not look like point-symmetry about center and another, though weak, hydraulic jump is shown in the lower/right corner.

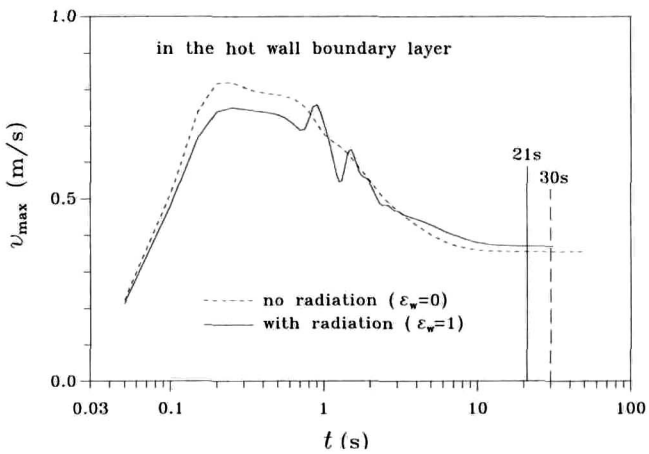

Fig. 4. Transient variation of the maximum velocity for the case with/without radiation

When the surface radiation is taken into consideration, the temporal variations of velocity vector and isotherm are plotted in Fig. 3. The difference is quite apparent. Due to its direct radiative heating, both ceiling and floor are being heated earlier compared with the case without radiation. The walls then heat up nearby air by conduction. The thermal boundary layer is developing not only at the hot wall, but also at the insulated ceiling and floor (at

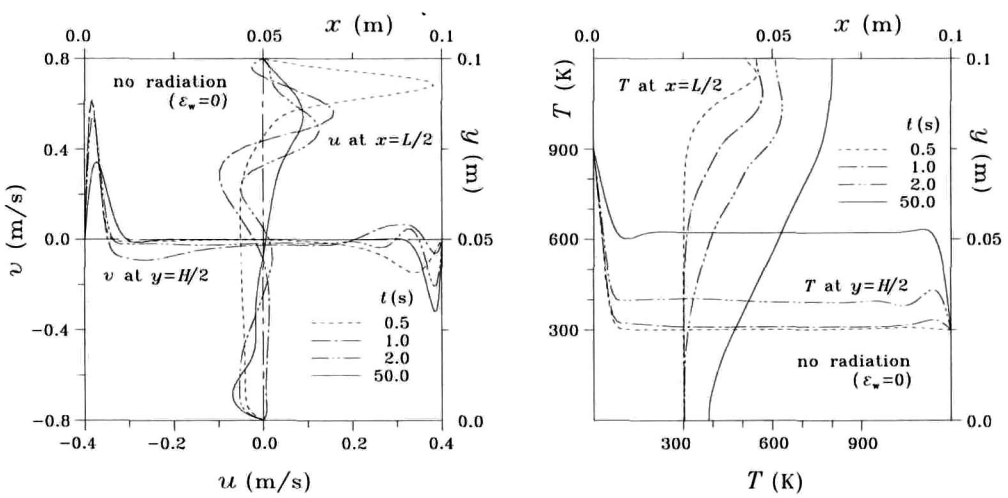

Fig. 5. Velocity and temperature profiles without radiation at x = L/2

0.2s). The hydraulic jump as well as the secondary cell appears in the upper/left corner in the same manner as in the case without radiation. At $t=0.6$s another counterclockwise secondary cell is formed in the lower/left corner as the flow is about to surge from the floor. The air above the floor is continuously heated and rises upward through 1.1s. A rising current from the floor provokes two secondary recirculating cells on both sides. The left-hand side cell disappears as the right-hand one is getting bigger by influx of air along cold right-hand side wall (at 1.3s). Since then, the remaining cell also disappears and the flow pattern becomes stabilized after $t=4.0$s. According to the criterion of steady state, it takes about 21s for the flow to be steady state, less than the case without radiation. At the steady state the temperature gradient over the floor is much steeper, which is apparently different from the one neglecting radiation. Also therein much higher is the flow velocity.

The transient variation of maximum velocity is illustrated in Fig. 4 and its position in the flow-field is denoted by the circle at each time in Fig. 2 and 3. The maximum velocity always occurs in the vicinity of the hot wall and its position moves downward as time passes. The maximum velocity increases till 0.2s and then decreases until the steady state is approached whether the radiation is considered or not. However, in the case with radiation the maximum velocity is seen to fluctuate from 0.8s to 2.5s, during which the air is rising up from the bottom floor.

The temporal plots of velocity and temperature distribution at $x=L/2$ and $y=H/2$ are illustrated in Fig. 5 (without radiation) and Fig. 6 (with radiation). Usually the vertical velocity is larger than the horizontal velocity, which is very irregular. Whereas the temperature gradient at ceiling as well as floor is zero because of the adiabatic condition (Fig. 5 (b)), it is non-zero once the radiation is involved (Fig. 6 (b)), since the sum of conductive and radiative heat fluxes is zero for adiabatic condition. As shown in Fig. 6 (b), the temperature gradient at the floor is always negative, but at the ceiling it is changing from negative to positive. In other words the ceiling is initially radiatively heated and then later it radiatively cools down. But the floor is always radiatively heated.

To investigate the heat transfer characteristics, following mean Nusselt numbers are defined at each surface.

$$\overline{Nu}_{hot,cold}^{T} = \overline{Nu}_{hot,cold}^{C} + \overline{Nu}_{hot,cold}^{R} = \frac{L}{H}\int_{o}^{H} \frac{q_w^C + q_w^R}{\lambda_0}(T_h - T_0)dy \qquad (15)$$

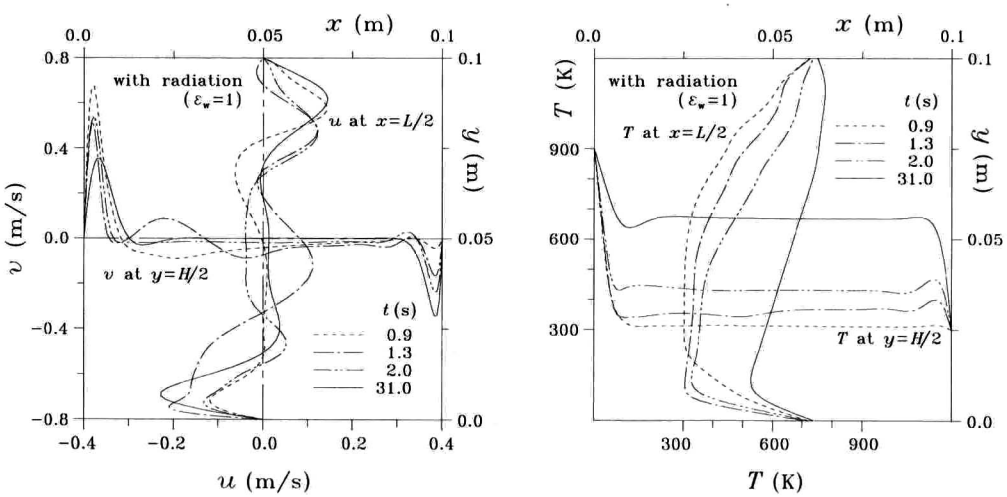

Fig. 6. Velocity and temperature profiles with radiation at x = $L/2$

$$\overline{Nu}^{\,C}_{ceilng,floor} = -\overline{Nu}^{\,R}_{ceilng,floor} = \int_o^H \frac{q^{\,C}_w}{\lambda_0(T_h - T_0)}\,dy \tag{16}$$

$$\overline{Nu}^{\,T}_{net} = \overline{Nu}^{\,T}_{hot} + \overline{Nu}^{\,T}_{cold} \tag{17}$$

The superscripts T, C, and R denote the total, conductive, and radiative terms, respectively.

Figure 7 illustrates a transient variation of total mean Nusselt number versus time on a logarithmic scale at both hot and cold wall. usually the total mean Nusselt number with radiation is higher than that without radiation. At the steady state the heat supplied from the hot wall is exactly balanced by the heat loss toward the cold wall, for the ceiling and the floor are adiabatic. therefore the total mean Nusselt number at the hot wall becomes equal to that with negative sign at the cold wall. In order to investigate the detailed heat transfer at each surface, the transient mean Nusselt numbers by the conduction are plotted in Fig. 8. It is not until the heated air arrives at the upper part of cold wall (at 0.5s) that $\overline{Nu}^{\,C}_{cold}$ slightly decreases for the case without radiation. When radiation is included, the small conductive heat loss is observed from the starting point since the cold wall is instantly heated by radiation from the other wall. As the heated air originating from the hot wall reaches the cold wall. the conductive heat loss increases. At the steady state the conduction occupies only 14.4% of the total

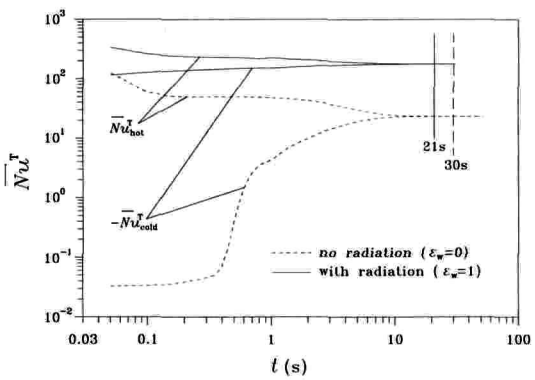

Fig. 7. Transient variation of total mean Nusselt number at both the hot wall and the cold wall for the case with/without radiation

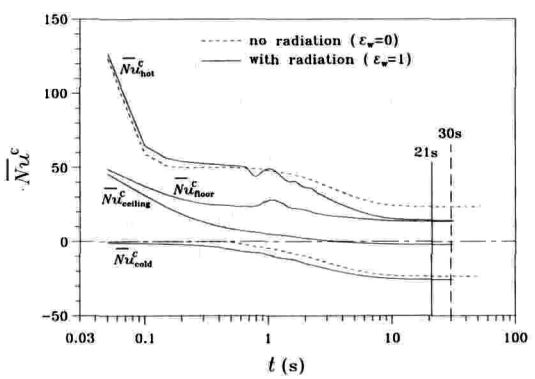

Fig. 8. Transient variation of conductive mean Nusselt number at all walls for the case with/without radiation

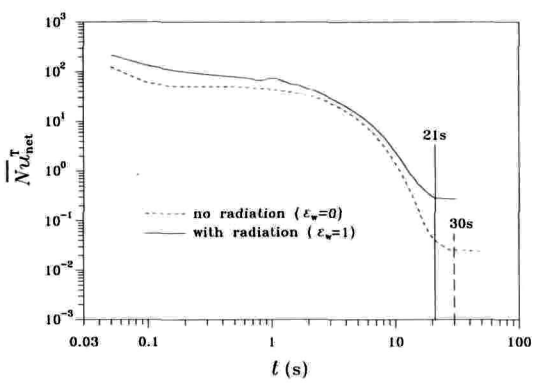

Fig. 9. Transient variation of net mean Nusselt number for the case with/without radiation

amount of heat supplied to the cold wall. there is a large decrease in the profile of $\overline{Nu}^{\,C}_{hot}$ when the hot wall supplies most of heat by the impulsive natural convective flow. During 0.8~2.5s the air near the hot wall is affected by the secondary cells. Therefore, the irregular fluctuation of $\overline{Nu}^{\,C}_{cold}$ is observed. At hot wall only 8.1% of heat is transferred to air by conduction at the steady state. While absolute value of $\overline{Nu}^{\,C}_{cold}$ is always larger for the case with radiation, $\overline{Nu}^{\,C}_{hot}$ with radiation is initially higher and then becomes smaller later. It results from the fact that the average temperature of enclosed air is higher with

radiation than otherwise. Without radiation there is no conductive heat flux at both adiabatic ceiling and floor irradiate exactly the same amount of the heat supplied by conduction. Figure 9 shows a transient variation os the net Nusselt number in the enclosure. A small fluctuation in the figure also results from the secondary cells. Because the radiation promotes the heat exchange in the enclosure, $\overline{Nu}_{net}^{C}$ is always higher with radiation.

Conclusions

An evolution of thermo-fluid field in the rectangular enclosure by a hot wall has been numerically investigated. Especially the effect of the surface radiation was examined in detail. Temperature dependency of the properties of air as well as the full compressibility due to temperature change was fully accounted for.

Rapid heating of both the adiabatic ceiling and the floor by incident radiation from the hot wall was found to render the evolution of thermo-fluid field unstable in the initial period. Therefore, secondary cells were induced by the uprising flow from the floor. Later these cells were merged into one and then disappeared as the steady state was approached. As a result, some fluctuation was observed in the overall heat transfer characteristics for a certain time. Ultimately the radiation was found to augment the heat transfer rate, which led to reduce the time required for the flow to reach the steady state.

At the steady state two hydraulic jumps were vividly discerned in upper/left as well as in lower/right corner for the case without radiation. However, the one in the lower/right corner could not be detected for the case with radiation, since the downward momentum along the left-hand cold wall could smoothly be taken up by the relatively fast flow over the bottom wall.

Usually the total mean Nusselt number with radiation was higher than that without radiation.

References

1. A. E. Gill, 1966, "The boundary-layer regime for convection in a rectangular cavity," *J. Fluid Mech.*, Vol. 26, No. 3, pp. 515-536

2. S. J. M. Linthorst, W.M.M. Schinkel, and C. J. Hoogendoorn, 1981, "Flow structure with natural convection in inclined air-filled enclosure," *J. Heat Transfer*, Vol. 103, pp. 535 -539

3. P. G. Simpkins and T. D. Dudderar, 1981, "Convection in rectangular cavities with differentially heated end walls," *J. Heat Transfer*, Vol. 110, pp. 433-456

4. S. M. ElSherbiny, K. G. T. Hollands, and G. D. Raithby, 1982, "Effect of thermal boundary layer conditions on natural convection in vertical and inclined air layer," *J. Heat Transfer*, Vol. 104, pp. 515-520

5. G. D. Mallinson, 1987, "The effects of side-wall conduction on natural convection in a slot," *J Heat Transfer*, Vol. 109, pp. 419-526

6. J. C. Patterson and J. Imberger, 1980, "Unsteady natural convection in a rectangular cavity," *J. fluid Mech.*, Vol. 100, No. 1, pp. 65-86

7. K. Kublbeck, G. P. Merker, and J. Straub, 1980, "Advanced numerical computation of two-dimensional time-dependent free convection in cavities," *Int. J. Heat Mass Transfer*, Vol. 23, pp. 203-217

8. J. C. Patterson, 1984, "On the existence of an oscillatory approach to steady natural convection in cavities," *J. Heat Transfer*, Vol. 106, pp. 104-108

9. G. N. Ivey, 1984, "Experiments on transient natural convection in a cavity," *J. Fluid Mech.*, Vol. 144, pp. 389-401

10. W. J. Hiller, St. Koch, T. A. Kowalewski, and F. Stella, 1993, "Onset of natural convection in a cube," *Int. J. Heat Mass Transfer*, Vol. 36, No. 13, pp. 3251-3263

11. K. S. Chen, J. R. Ho, and J. A. C. Humphrey, 1987, "Steady, two-dimensional, natural convection

in rectangular enclosure with differently heated walls," *J. Heat Transfer*, Vol. 109, pp. 400-406

12. J. L. Zia, M. D. Xin, and H. J. Zhang, 1990, "Natural convection in an externally heated enclosure containing a local heat source," *J. Thermophysics*, Vol. 4, No. 2, pp. 233-238

13. M. Hasnaoui, E. Bilgen, and P. Vasseur, 1992, "Natural convection heat transfer in rectangular cavities partially heated from below," *J. Thermophysics*, Vol. 6, No. 2, pp. 255-264

14. D. W. Larson and R. Viskanta, 1976, "Transient combined laminar free convection and radiation in a rectangular enclosure," *J. Fluid Mech.*, Vol. 78, pp. 65-85

15. H. Hilsenrath et al., 1960, *Tables of Thermodynamics and Transport Properties of Air, Argon, Carbon Dioxide, Hydrogen, Oxygen, and Steam*, Pergamon Press, New York

16. R. Siegel and J. R. Howell, 1981, *Thermal Radiation Heat Transfer*, McGraw-Hill, New York

17. T. Hayase, J. A. C. Humphrey, and R. Greif, 1992, "A consistently formulated QUICK scheme for fast and stable convergence using finite-volume iterative calculation procedures," *J. Comput. Phys.*, Vol. 98, pp. 108-118

18. S. V. Partankar, 1980, *Numerical Heat Transfer and Fluid Flow*, McGraw-Hill, New York